







[dx.doi.org/10.17488/RMIB.45.2.2](https://dx.doi.org/10.17488/RMIB.45.2.2)

E-LOCATION ID: 1409

## Involvement of the Lung Parenchyma Analyzed by Frequency Components of the Tidal Volume Assessed by Electrical Bioimpedance

### Afectación del Parénquima Pulmonar Analizada por Medio de las Componentes de Frecuencia del Volumen Tidal Evaluado por Bioimpedancia Eléctrica

Francisco Miguel Vargas Luna<sup>1</sup> , María Isabel Delgadillo Cano<sup>1</sup> , Pere Joan Riu Costa<sup>2</sup> , Svetlana Kashina<sup>1</sup>   
José Marco Balleza Ordaz<sup>1</sup>  

<sup>1</sup>Universidad de Guanajuato - México

<sup>2</sup>Universitat Politècnica de Catalunya, Electronics and Biomedical Instrumentation Department, Barcelona - Spain

#### ABSTRACT

Pulmonary function tests are vital for detecting pathologies, especially chronic obstructive pulmonary diseases (COPD), emphasizing the importance of assessing lung parenchyma involvement in maintaining proper gas exchange. Electrical impedance tomography (EIT) offers a non-invasive alternative for respiratory function evaluation while preserving natural breathing. We propose using EIT to detect lung parenchyma conditions by analyzing tidal volume patterns (by averaging the impedance image) in the frequency domain. Twenty COPD patients underwent simultaneous evaluation with a pneumotachometer and an EIT device, performing three 30-second respiratory maneuvers. FFT spectra analysis yielded parameters, including the area under the curve and quartiles (25 %, 50 %, 75 %) of power values in six frequency regions. Correlations between these parameters and clinical test results (pulmonary diffusing capacity and arterial blood gas analysis) revealed significant associations, particularly with PCO<sub>2</sub>. Multiple linear regression analysis predicted PCO<sub>2</sub> with an  $R^2_{adj} = 0.827$ , suggesting the potential for non-invasively detecting lung parenchyma affectation by correlating FFT bioimpedance ventilatory patterns with gas exchange performance in COPD patients.

**KEYWORDS:** COPD, electrical impedance tomography, lungs, pulmonary function testing

## RESUMEN

Las pruebas de función pulmonar son fundamentales para detectar patologías, especialmente enfermedades pulmonares obstructivas crónicas (EPOC), destacando la importancia de evaluar la participación del parénquima pulmonar en el mantenimiento adecuado del intercambio gaseoso. La tomografía por la bioimpedancia eléctrica (TIE) ofrece una alternativa no invasiva para la evaluación de la función respiratoria mientras se conserva la respiración natural. Proponemos utilizar la TIE para detectar condiciones del parénquima pulmonar mediante el análisis de patrones de volumen tidal en el dominio de frecuencia. Veinte pacientes con EPOC fueron evaluados simultáneamente con un neumotacómetro y un dispositivo de TIE, realizando tres maniobras respiratorias de 30 segundos cada una. El análisis de espectros FFT proporcionó parámetros, incluyendo el área bajo la curva y los cuartiles (25 %, 50 %, 75 %) de los valores de potencia en seis regiones de frecuencia. Las correlaciones entre estos parámetros y los resultados de pruebas clínicas (capacidad de difusión pulmonar y análisis de gases en sangre arterial) revelaron asociaciones significativas, especialmente con PCO<sub>2</sub>. El análisis de regresión lineal múltiple predijo PCO<sub>2</sub> con un  $R^2_{adj} = 0.827$ , sugiriendo la posibilidad de detectar de manera no invasiva la afectación del parénquima pulmonar al correlacionar los patrones ventilatorios de bioimpedancia FFT con el rendimiento del intercambio gaseoso en pacientes con EPOC.

**PALABRAS CLAVE:** EPOC, pulmón, test de funciones pulmonares, tomografía por impedancia eléctrica

### Corresponding author

TO: José Marco Balleza-Ordaz

INSTITUTION: Universidad de Guanajuato - México

ADDRESS: Loma del Bosque #103, Lomas del Campestre,  
37150 León de los Aldama, Guanajuato, Mexico.

EMAIL: [jm.balleza@ugto.mx](mailto:jm.balleza@ugto.mx)

### Received:

22 November 2023

### Accepted:

7 April 2024

## INTRODUCTION

The importance of diagnosing lung function lies in determining whether patients exhibit a restrictive, obstructive, or restrictive-obstructive respiratory pattern through the interpretation of measurements depicting dynamic or static lung performance <sup>[1]</sup>. There are four clinical trials to diagnose respiratory patterns in patients: a) spirometry, b) static lung volumes, c) lung's ability to diffuse carbon monoxide, and d) 4 examination of blood gas <sup>[1]</sup>. All of these are used to diagnose and monitor the severity level of pulmonary diseases such as chronic obstructive pulmonary disease (COPD). COPD is a prevalent, avoidable, and manageable condition marked by persistent respiratory symptoms and restricted airflow resulting from abnormalities in the airways and/or alveoli, typically stemming from substantial exposure to harmful particles or gases <sup>[2][3][4]</sup>. Since the appearance of SARS-CoV-2 (COVID-19), the performance of the four clinical trials has become a complicated routine not only for COPD diagnosis but also for COPD patients with SARS-CoV-2. Nowadays, the main risk of conducting these tests is COVID-19 transmission due to contamination of materials used during each procedure <sup>[4][5][6]</sup>, increasing the probability of developing severe lung disease or death.

Electrical Impedance Tomography (EIT) is a radiation-free and non-invasive method employed for visualizing the distribution of impedance in specific regions across the cross-sectional human body <sup>[7][8]</sup>. EIT frames are reconstructed from a set of impedance measurements obtained by an arrangement of 16 electrodes placed around the thorax at the level of the sixth intercostal space <sup>[9][10][11]</sup>, registering impedance changes that allow the characterization of internal movements produced by the human body. Some EIT applications in pneumology include: 1) estimation of regional lung perfusion <sup>[12][13]</sup>, 2) regional lung ventilation characterization in patients with pulmonary fibrosis <sup>[14]</sup> and pulmonary hypertension <sup>[15]</sup>, 3) detection of bronchopulmonary dysplasia in neonates at early stages <sup>[16]</sup>, 4) ventilatory pattern monitoring in patients diagnosed with sudden onset of respiratory distress syndrome (ARDS) <sup>[17]</sup>, 5) evaluation of an effect of pleural effusion drainage in patients submitted to mechanical ventilation <sup>[18]</sup>, among others.

EIT applications in COPD patients aim to monitor parameters that describe temporal changes in pulmonary airflow limitation. For example, Milne *et al.* (2019) proposed using EIT to characterize ventilatory heterogeneity (VH) using lung tidal volume changes. In this case, EIT determinations were compared with the forced oscillation technique (FOT) in COPD patients compared with a control group. Three parameters from bioimpedance changes corresponding to each voxel of the EIT image were calculated. The first one was the mean expiratory time. The second measure involved calculating the average time gap between the impedance alterations in individual voxels and the overall impedance variation in the entire EIT image or phase shift. The third one was the mean amplitude of impedance signals determined by each EIT voxel. The coefficient of variation (VC) and index of heterogeneity (HI) for each parameter were calculated to quantify lung impedance distribution: the coefficient of variation (CV) and the heterogeneity index (HI). A HI is the CV of the region defined by the 28 near neighboring voxels of the point considered. The HI is defined as the mean value of all local HI for the whole EIT image. From the obtained results, both CV and HI evidenced a significant increase in COPD patients compared with the control. All assessments were linked to spirometry parameters and measurements of resistance and reactance in the Forced Oscillation Technique (FOT), revealing statistically significant distinctions between the groups <sup>[19]</sup>.

Karagiannidis *et al.* (2018) suggested employing EIT to ascertain regional expiratory time constants in intubated patients with COPD and ARDS. These time constants were calculated based on the overall impedance signal obtained

from EIT. These parameters were compared with lung volume signals obtained by a pneumotachograph. Authors evidenced a significant correlation, roughly 80 %, between EIT-derived time constants and those obtained by a pneumotachometer <sup>[20]</sup>.

Vogt *et al.* (2016) suggested utilizing EIT to observe the spatial and temporal distribution of ventilation (VD) in COPD patients while under the influence of an inhaled bronchodilator. In this study, spirometry served as the gold standard. The EIT image values corresponding to various spirometry parameters were identified, including FEV<sub>1</sub>, FVC, FEV<sub>1</sub>/FVC, tidal volume, peak flow, and mean forced expiratory flow between 25 and 75 % of FVC (FEF<sub>25-75</sub> %). The FEV<sub>1</sub>/FVC ratio was used to assess the bronchodilator's impact on spatial ventilation distribution. A significant bronchodilator response was evidenced in most of the patients assessed by these EIT parameters <sup>[21]</sup>.

In the above-mentioned studies, authors used EIT as an alternative method to monitor parameters that describe lung function. These parameters were compared with those obtained by different clinical trials. EIT utilizes frequency analysis to interpret signals, but correlating FFT frequencies with respiratory parameters remains challenging. EIT captures impedance variations within a body, offering insights into lung function. However, the exact correspondence between FFT peaks and specific respiratory metrics remains elusive. Despite advancements, establishing a direct correlation remains complex due to the multifactorial nature of physiological processes and signal intricacies. New research is needed to fully unveil these connections, enabling precise respiratory parameter estimations. Bridging this gap promises enhanced diagnostic capabilities and refined monitoring techniques, driving EIT towards more accurate and insightful clinical applications in respiratory care.

This study proposes to analyze the frequency of electrical bioimpedance changes in the ventilation pattern with those parameters corresponding to clinical procedures, mainly diffusing lung capacity trials and arterial blood gas tests in a group of COPD patients. We hypothesize that EIT supplies information about lung airflow limitation through the frequency analysis of tidal-volume respiration signals. The main objective of this research is to identify frequency components of the tidal volume lung signal obtained by EIT and correlate them with parameters of the pulmonary trials in a group of COPD patients to detect lung parenchyma involvement.

## MATERIALS AND METHODS

### Instrumentation

The TIE4-sys represents the fourth iteration of an EIT prototype developed at the Department of Electronic Engineering, Universitat Politècnica de Catalunya, Barcelona, Spain. This system features 16 electrodes positioned around the thoracic box at the sixth intercostal space, aligning with the established protocol of our research group <sup>[22]</sup>. The process involves injecting a 1 mA electrical current at 48 kHz through a pair of adjacent electrodes, with the resulting differential voltage recorded at the rest of the adjacent electrode pairs. Following the completion of potentials for a specific injection pair, the injection point is shifted to the next adjacent electrode pair, initiating a new cycle of measurements <sup>[23]</sup>. The entire procedure concludes when all adjacent electrode pairs have been employed as injectors. EIT determinations are redundant, enabling the estimation of the reciprocity error <sup>[24]</sup>. This parameter characterizes systematic errors and malfunctions that may arise during the procedure, such as inadequate contact between electrodes and the skin <sup>[25][26]</sup>.

The TIE4-sys reconstruction algorithm utilized for image generation is a weighted back-projection algorithm. The

software incorporates a weight matrix that considers the spatial sensitivity of each pixel in the EIT image <sup>[27][28]</sup>. The TIE4-sys scan rate is 17 images/s <sup>[25]</sup>. Dynamic images are relative impedance changes calculated using a baseline (BL) as a reference. The BL of TIE4-sys is composed of averaging 204 images corresponding to 12 seconds of acquisition <sup>[25]</sup>.

Following the recording of the breathing pattern and the generation of dynamic images, an impedance signal ( $\Delta Z$ ) is obtained by determining the variance between the average impedance of an Electrical Impedance Tomography (EIT) image and the baseline (BL). The parameter  $\Delta Z$  is computed for each of the 510 EIT images, corresponding to a 30-second monitoring period with TIE4sys.

For monitoring lung tidal volume, the pneumatometer employed was a Med Graphics preVent™ Pneumotach provided by Medical Graphics Corporation (St. Paul, MN, USA). The device is controlled by software supplied by the manufacturer, recording measurements displayed graphically on the screen and numerically downloadable as a text file. Calibration of the pneumotachometer was performed using a 3-L syringe following standard laboratory protocols, establishing it as the gold standard for measurements <sup>[29]</sup>.

## Participants

A group of 20 male patients (Caucasic, age  $67 \pm 9$ ), all diagnosed with COPD at the Pneumology Department of Hospital de la Santa Creu I Sant Pau, Barcelona, Spain, was analyzed. In general, all patients showed an intense obstructive ventilatory alteration (FEV1/FVC roughly  $45 \% \pm 11 \%$ ) and a moderate level of air trapping (RV/TLC roughly 1.4) <sup>[30]</sup>. The prevalence of COPD in the countries of the European Union is higher in men than in women by approximately 30 % <sup>[31]</sup>. Due to this fact, this study was conducted on male subjects. All clinical procedures were performed between 9 am and noon in a quiet room at sea level with an ambient temperature of 25 °C and a relative humidity of 60 %. All patients voluntarily consented to participate in the study, which had been previously approved by the institutional ethics committee. A written informed consent was read and signed by all participants. This research was conducted according to the guidelines outlined in the Declaration of Helsinki <sup>[32]</sup>.

## Clinical Tests

The medical history of the COPD patients included at least one of the four clinical procedures of interest for our study: 1) spirometry, 2) static lung volumes, 3) carbon monoxide diffusing capacity in the lungs, 4) analysis of blood gases. Spirometry is used to screen for abnormalities of airflow or lung volume <sup>[33][34]</sup>. The variables obtained from this test are forced vital capacity (FVC), forced expiratory volume in the first second (FEV1), and the FEV1/FVC ratio. All patients had spirometry test parameters. Static lung volume test assesses air trapping in the lungs. The parameters from this test are residual volume (RV) and total lung capacity (TLC) <sup>[35]</sup>. Out of the 20 COPD patients, only 15 participants had this test available. Pulmonary diffusing capacity for carbon monoxide test measures gas transferred from the alveoli to the capillary blood per unit time <sup>[36]</sup>. The variables obtained from this test are pulmonary diffusing capacity for carbon monoxide (DLCO), pulmonary diffusing capacity adjusted to hemoglobin (DLCOAdj), and the ratio DLCO/Av (Av: alveolar volume). In this case, out of the 20 patients, only 16 had results from this procedure available. Finally, the arterial blood gas analysis gives information about the partial pressures of gas in blood and acid-base content <sup>[37]</sup>. The parameters measured in this test include the partial pressure of oxygen in arterial blood (PO<sub>2</sub>) and the partial pressure of carbon dioxide in arterial blood (PCO<sub>2</sub>). From the group of patients, only 14 had results from this analysis.

## Procedure

All determinations analyzed in this study were previously used to obtain and assess a set of calibration equations to convert EIT signals into measurable volume signals <sup>[38][39]</sup>. In this study, two devices were used: the pneumotachometer and TIE4-sys. Both devices were simultaneously connected to each patient; the pneumotachometer through a mouthpiece and clip nose and TIE4-sys through 16 electrodes (Red Dot 2560-3M, London, Ontario, Canada) placed at the level of the sixth intercostal space, making a 224 pixel mesh. At this level of the thorax, the bioimpedance changes corresponding to lung tidal volume are not affected <sup>[40][41]</sup>. The pneumotachometer is used to quantify pulmonary airflow, meanwhile, TIE4-sys monitors bioimpedance changes corresponding to lung volume variations. Three respiratory exercises under tidal volume conditions were recorded for each patient. Each respiratory maneuver was performed by each volunteer adopting a sitting position and lasted 30 seconds with three minutes of rest between measurements. The sitting position contributes to reducing strain on the body during respiration and reduces the wear and tear on the joints, muscles, and ligaments <sup>[42]</sup>. Figure 1 shows the electrodes' placement and a typical image obtained by EIT.

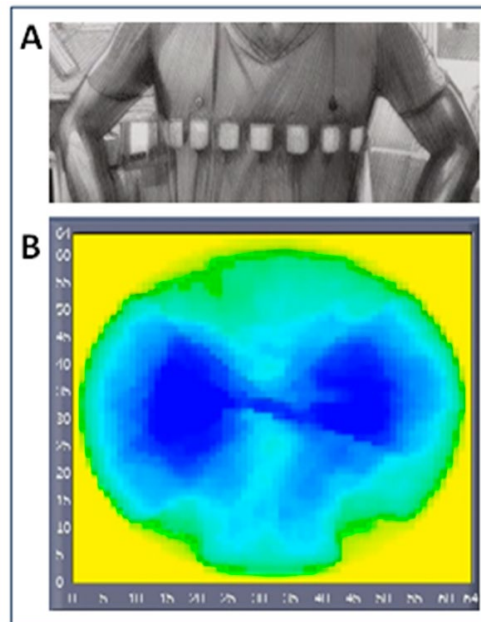


FIGURE 1. A) Electrodes' placement on the thorax; B) Typical EIT image

## Signal Processing

The three bioimpedance signals include 30 seconds with a scan rate of 17 samples/s, which is 510 points for each one. Each pneumotachometer signal data encompasses 30 seconds with a scan rate of 50 samples/s, that is 1500 points. The tidal volume determinations and bioimpedance changes corresponding to each respiratory maneuver were estimated using the differences between each maximum and the following minimum values of each signal. MatLab software was used to perform the signal processing and statistical analysis. From the analysis of FFT graphs, six regions from the signal spectrum (R1 - R6) are considered for analysis: R1 is defined from 0 to 200 mHz, R2 from 200 mHz to 400 mHz, R3 from 400 mHz to 600 mHz, R4 from 600 mHz to 800 mHz, R5 is between 800 mHz and 1 Hz, and R6 covers the frequencies higher than 1 Hz. Four parameters were estimated from each frequency region and for each patient: the mean area under the curve (Ri-A from the three maneuvers), and the quartile at 25 %, 50 %, and 75 % of FFT-Spectrum data (Ri-Q1, Ri-Q2, and Ri-Q3 respectively by merging the three data sets).

## Statistical Analysis

The utilization of quartile analysis was implemented due to the non-normal distribution observed in the majority of frequency segment data, as indicated by the Shapiro-Wilk test ( $p$ -value  $< 0.05$ ). Following this, these parameters were correlated with the results from clinical tests, primarily focusing on pulmonary diffusing capacity for carbon monoxide and arterial blood gas analysis, but also including spirometry and static lung volumes <sup>[43][44]</sup>.

The tidal volumes obtained by the pneumotachometer technique, and those volumes estimated by EIT data show normal distribution; therefore, the correlation between tidal volumes and bioimpedance changes was performed by parametric Pearson correlation. However, the correlations between the parameters (areas under the curve and quartiles) estimated in each segment of FFT spectrums and those obtained by clinical tests were performed by a Spearman correlation because most of the FFT parameters do not have a normal distribution.

## RESULTS AND DISCUSSION

It is known that bioimpedance changes due to respiration vary greatly between persons. Even one person may present different results due to, for example, hydration status. For that reason, in the present study, we have not chosen a study-control group approach, but the frequency variations were directly correlated with the parameters obtained in clinical tests. The correlation between tidal volume measurements obtained by the pneumotachometer and electrical bioimpedance change determinations for all the participants was over 95 % (Pearson  $r$ ,  $p$ -value  $< 0.05$ ).

Most of the data parameters corresponding to segmented FFT-Spectrum (Parameters from regions 1, 3, 5, 6, and R4-Q1 and R4-Q2) did not follow a normal distribution in the electrical bioimpedance spectrum (S-W,  $p$ -value  $< 0.05$ ). The correlations between these parameters and clinical evaluations are performed by the Spearman rank correlation test ( $\rho$ ,  $p$ -values  $< 0.05$ ). The parameter PCO<sub>2</sub> shows significant correlations with the following electrical bioimpedance FFT parameters: R3-A with a correlation  $\rho = -0.564$  ( $p=0.036$ ), R4-A with a correlation  $\rho = -0.666$  ( $p=0.009$ ), R5-A with a correlation  $\rho = -0.635$  ( $p=0.015$ ), and R6-A with a correlation  $\rho = -0.586$  ( $p=0.028$ ). Also, this parameter shows a significant correlation with quantile values of FFT data at the same regions: R3-Q3,  $\rho = -0.686$  ( $p=0.007$ ), R4-Q1, R4-Q2, R4-Q3 with  $\rho = -0.533$  ( $p=0.05$ ),  $\rho = -0.560$  ( $p=0.037$ ),  $\rho = -0.648$  ( $p=0.012$ ) respectively; R5-Q1, R5-Q2, R5-Q3 with  $\rho = -0.626$  ( $p=0.017$ ),  $\rho = -0.611$  ( $p=0.02$ ),  $\rho = -0.569$  ( $p=0.034$ ) respectively; and R6-Q3,  $\rho = -0.584$  ( $p=0.028$ ). Residual volume (RV) correlates with impedance R2-Q1  $\rho = -0.595$  ( $p=0.019$ ). Also, DLCO<sub>adj</sub> correlates with R4-Q1 and R4-Q2,  $\rho = 0.506$  ( $p=0.045$ ) and  $\rho = 0.512$  ( $p=0.043$ ) respectively (Table 1, Table 2, Table 3).

**TABLE 1. Spearman correlations of partial areas under FFT spectrum in different frequency ranges of electrical bioimpedance signal and PCO<sub>2</sub>.**

Electrical bioimpedance region area	Correlation with PCO <sub>2</sub> : $\rho$ (p)
R3	-0.564 (0.036)
R4	-0.666 (0.009)
R5	-0.635 (0.015)
R6	-0.586 (0.028)

**TABLE 2. Spearman correlation of PCO<sub>2</sub>, RV and DLCOadj with quantiles of power values of FFT spectrum in different frequency ranges of bioimpedance signal.**

Electrical bioimpedance region-quartile	Correlation with PCO <sub>2</sub> : $\rho(p)$	Correlation with RV: $\rho(p)$	Correlation with DLCOadj: $\rho(p)$
R2-Q1		-0.595 (0.019)	
R3-Q3	-0.686 (0.007)		
R4-Q1	-0.533 (0.05)		0.506 (0.045)
R4-Q2	-0.560 (0.037)		0.512 (0.043)
R4-Q3	-0.648 (0.012)		
R5-Q1	-0.626 (0.017)		
R5-Q2	-0.611 (0.02)		
R5-Q3	-0.569 (0.034)		
R6-Q3	-0.584 (0.028)		

**TABLE 3. Spearman correlation of PCO<sub>2</sub> and PO<sub>2</sub> with quantiles of power values of FFT spectrum in different frequency ranges of Pneumotachometer signal.**

Pneumotac region-quartile	Correlation with PCO <sub>2</sub> : $\rho(p)$	Correlation with PO <sub>2</sub> : $\rho(p)$
R2-Q1		0.682 (0.007)
R2-Q3	-0.540 (0.046)	
R4-Q1	-0.560 (0.037)	

Based on these results, multiple linear regression was calculated with PCO<sub>2</sub> as a dependent variable and the significantly correlated areas and quartiles as predictors, obtaining an expression with the most significant coefficients (9 predictors: R3-A, R4-A, R5-A, R6-A, R3-Q3, R4-Q1, R4-Q2, R6-Q3, R5-Q2). This multiple regression has an  $R^2=0.947$  with an  $R^2_{adj}=0.827$  (Figure 2).

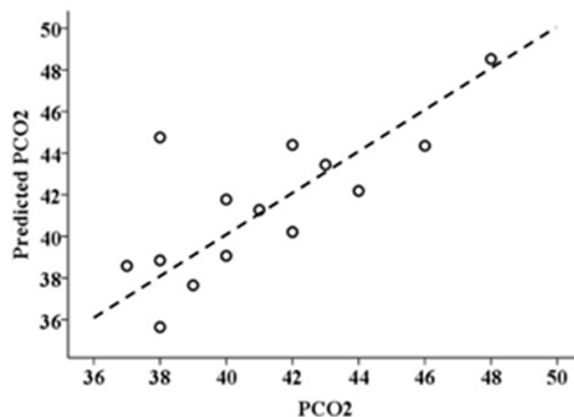


**FIGURE 2. Dispersion graph of predicted PCO<sub>2</sub> obtained by multiple regression ( $R^2=0.947$  with an  $R^2_{adj}=0.827$ ) and the value measured by arterial gas exchange analysis.**

Pneumotachometer FFT parameters correlate mainly with spirometry results, as was discussed in other investigations. PCO<sub>2</sub> correlates with R2-Q3 and R4-Q1 with  $\rho = -0.540$  ( $p=0.046$ ) and  $\rho = -0.560$  ( $p=0.037$ ) respectively, and R2-Q1 correlates with PO<sub>2</sub> with  $\rho = 0.682$  ( $p=0.007$ ).



This research aimed to detect lung parenchyma involvement by electrical impedance tomography in a group of COPD patients. To achieve this goal, it was proposed to analyze the frequency spectrum (FFT-module) of the bioimpedance signal obtained by EIT, under lung tidal volume conditions. Each FFT spectrum was segmented into six frequency ranges, in which four parameters of interest (area under each range of FFT spectrum, and quartile at 25 %, 50 %, and 75 % of FFT data in each range) were estimated. These parameters were correlated with those resulting from four clinical tests involved with the gas exchange condition, mainly with arterial blood gas parameters.

The normal respiration frequency lies in the first and sometimes second defined range frequencies (< 400 mHz). It is proposed that high-frequency ranges defined involve the noise coming from parenchyma involvement and that this is detected better with the electrical bioimpedance technique. Low frequency (< 4Hz) Forced Oscillation Lung Function Test has been related to viscoelastic properties of parenchyma <sup>[45]</sup>, so our claim can be understood as a way to relate parenchyma involvement with low-frequency features of tidal volume (> 0.4 Hz corresponding to what we call high-frequency range) While the exact relationship between the involvement of lung parenchymal and bioimpedance is complex and not fully elucidated, it's clear that alterations in lung parenchymal properties can potentially affect bioimpedance measurements. This highlights the importance of considering various physiological factors when interpreting bioimpedance data in the context of lung function assessment or disease diagnosis. In this study, the highest correlations of bioimpedance areas and quartiles of the FFT spectrum at high frequencies (higher than 400 mHz) were those corresponding to the parameters of arterial blood gas technique, mainly PCO<sub>2</sub>. This correlation is negative, implying that the higher FFT values of the high-frequency region, the lower PCO<sub>2</sub> determinations or better performance of the gas exchange. This parameter is important to determine the level of obstruction, restriction, or obstruction-restriction of the ventilatory pattern of a patient <sup>[1][2][3][4]</sup>. This could be possible because EIT detects the alteration of lung parenchyma through electrical current application and biopotential detection around the thorax. An explanation could be that during inhalation, alveoli expand to perform the gas exchange. These alveoli expansions produce high-frequency noise when this is electrically monitored. However, one COPD condition is the destruction of alveoli ramification (emphysema), including bronchioles <sup>[1][2][3][4]</sup>. We hypothesize that EIT detects the involvement of lung parenchyma (alveoli and bronchioles). The involvement of the parenchyma can be detected by the analysis of low frequencies features of the tidal volume obtained by the whole EIT image or by regions of interest.

It's crucial to emphasize that the results we've acquired are constrained to a group of 20 individuals with COPD. To enhance the robustness of future studies, it is essential to augment the size of the patient sample. As well as, to use regions of interest on EIT images and monitor the bioimpedance changes, analyzing its frequency components and correlating them with parameters of clinical tests.

## CONCLUSIONS

From the frequency analysis of an electrical bioimpedance signal obtained by EIT, under lung tidal volume conditions, it is possible to detect parameters of gas exchange conditions such as PCO<sub>2</sub> by analyzing frequency features at high frequencies from the FFT spectrum. Therefore, based on the sample of patients, it is possible to detect the level of affectation of the ventilatory pattern. Likewise, using EIT, we can predict the performance level of gas exchange in a group of COPD patients with an intense obstructive ventilatory alteration and a moderate level of air trapping.

## ETHICAL STATEMENT

The clinical study in which the lung volumes and bioimpedance determinations were acquired in a group of COPD patients was approved by the Committee of Ethics of the Hospital de la Santa Creu i Sant Pau, Barcelona, Spain.

## ACKNOWLEDGMENTS

All authors thank Universidad de Guanajuato, Dirección de Apoyo a la Investigación y al Posgrado (DAIP) for financial support.

S. Kashina acknowledges CONAHCyT for her postdoctoral fellowship.

## DECLARATION OF INTERESTS

The authors declare that they have no known competing financial interests or personal relationships that could have appeared to influence the work reported in this paper.

## AUTHOR CONTRIBUTIONS

F. M. V. L. Data acquisition, data analysis and interpretation, and writing original draft. M. I. D. C. Data analysis and interpretation, review of the manuscript. P. J. R. C. Study design, data analysis and interpretation, and review of the manuscript. S. K. Study design, data acquisition, data analysis and interpretation, review of the manuscript, and funding acquisition. J. M. B. O. Study design, data acquisition, data analysis and interpretation, review of the manuscript, and funding acquisition. All authors approved the version to be published and agree to be accountable for all aspects of the work in ensuring that questions related to the accuracy or integrity of any part of the work are appropriately investigated and resolved.

## REFERENCES

- [1] B. H. Culver, "Pulmonary function testing," in *Clinical Respiratory Medicine*, S. G. Spiro, G. A. Silvestri, A. Agusti, Eds., Philadelphia, PA, United State: Elsevier, 2012, ch. 9, pp. 133-142.
- [2] A. Virani, S. Baltaji, M. Young, T. Dumont, T. Cheema, "Chronic Obstructive Pulmonary Disease: Diagnosis and GOLD Classification," *Crit. Care Nurs. Q.*, vol. 44, no. 1, pp. 9-18, Mar. 2021, doi: <https://doi.org/10.1097/CNQ.0000000000000335>
- [3] Global Initiative for Chronic Obstructive Lung Disease. "Global strategy for the diagnosis, management, and prevention of chronic obstructive pulmonary disease." Global Initiative for Chronic Obstructive Lung Disease: <https://goldcopd.org/wp-content/uploads/2019/12/GOLD-2020-FINAL-ver1.2-03Dec19-WMV.pdf> (accessed Sep. 28, 2023).
- [4] D. M. D. Halpin, G. J. Criner, A. Papi, D. Singh, et al., "Global Initiative for the Diagnosis, Management, and Prevention of Chronic Obstructive Lung Disease. The 2020 GOLD Science Committee Report on COVID-19 and Chronic Obstructive Pulmonary Disease," *Am. J. Resp. Crit. Care*, vol. 203, no. 1, pp. 24-36, 2021, doi: <https://doi.org/10.1164/rccm.202009-3533SO>
- [5] A. McGowan. "Recommendation from ERS Group 9.1 (Respiratory function technologists /Scientists) Lung function testing during COVID-19 pandemic and beyond." ERS. <https://ers.app.box.com/s/zs1uu88wy51monr0ewd990itoz4tsn2h>
- [6] M. C. McCormack, D. A. Kaminsky. "American Thoracic Society. Pulmonary function laboratories: Advice Regarding COVID-19." American Thoracic Society. <https://www.thoracic.org/professionals/clinical-resources/disease-related-resources/pulmonary-function-laboratories.php> (accessed Sep. 16, 2023).
- [7] F. A. Escobar Revelo, V. H. Mosquera Leyton, C. F. Rengifo, "Electrical Impedance Tomography: Hardware Fundamentals And Medical Applications," *Ing. Solidar.*, vol. 16, no. 3, pp. 2-29, 2020, doi: <https://doi.org/10.16925/2357-6014.2020.03.02> (accessed 2023).
- [8] T. A. Khan, S. H. Ling, "Review on electrical impedance tomography: Artificial intelligence methods and its applications," *Algorithms*, vol. 12, no. 5, pp. 70-88, 2019, doi: <https://doi.org/10.3390/a12050088>
- [9] P. Grasland-Mongrain, C. Lafon, "Review on Biomedical Techniques for Imaging Electrical Impedance," *IRBM*, vol. 39, no. 4, pp. 243-250, 2018, doi: <https://doi.org/10.1016/j.irbm.2018.06.001>
- [10] Z. Wang, S. Yue, H. Wang, Y. Wang, "Data preprocessing methods for electrical impedance tomography: a review," *Physiol. Meas.*, vol. 41, no. 9, art. no. 09TR02, 2020, doi: <https://doi.org/10.1088/1361-6579/abb142>

- [11] Z. Zong, Y. Wang, Z. Wei, "A Review of Algorithms and Hardware Implementations in Electrical Impedance Tomography," *Prog. Electromagn. Res.*, vol. 169, pp. 59-71, 2020, doi: <https://doi.org/10.2528/PIER20120401>
- [12] S. Yuan, H. He, Y. Long, Y. Chi, I. Frerichs, Z. Zhao, "Rapid dynamic bedside assessment of pulmonary perfusion defect by electrical impedance tomography in a patient with acute massive pulmonary embolism," *Pulm. Circ.*, vol. 11, no. 1, pp. 1-3, 2021, doi: <https://doi.org/10.1177/2045894020984043>
- [13] H. He, Y. Long, I. Frerichs, Z. Zhao, "Detection of acute pulmonary embolism by electrical impedance tomography and saline bolus injection," *Am. J. Resp. Crit. Care.*, vol. 202, no. 6, pp. 881-882, 2020, doi: <https://doi.org/10.1164/rccm.202003-0554IM>
- [14] E. Krauss, D. van der Beck, I. Schmalz, J. Wilhelm, et al., "Evaluation of Regional Pulmonary Ventilation in Spontaneously Breathing Patients with Idiopathic Pulmonary Fibrosis (IPF) Employing Electrical Impedance Tomography (EIT): A Pilot Study from the European IPF Registry (eurIPFreg)," *J. Clin. Med.*, vol. 10, no. 2, art. no. 192, 2021, doi: <https://doi.org/10.3390/jcm10020192>
- [15] M. Proença, F. Braun, M. Lemay, J. Solà, et al., "Non-invasive pulmonary artery pressure estimation by electrical impedance tomography in a controlled hypoxemia study in healthy subjects," *Sci. Rep.*, vol. 10, art. no. 21462, 2020, doi: <https://doi.org/10.1038/s41598-020-78535-4>
- [16] W. Onland, J. Hutten, M. Miedema, L. D. Bos, P. Brinkman, A. H. Maitland-van der Zee, A. H. van Kaam, "Precision Medicine in Neonates: Future Perspectives for the Lung," *Front. Pediatr.*, vol. 8, pp. 732-742, 2020, doi: <https://doi.org/10.3389/fped.2020.586061>
- [17] R. Cornejo, P. Iturrieta, T. M. Olegário, C. Kajiyama, et al., "Estimation of changes in cyclic lung strain by electrical impedance tomography: Proof-of-concept study," *Acta Anaesth. Scand.*, vol. 65, no. 2, pp. 228-235, 2021, doi: <https://doi.org/10.1111/aas.13723>
- [18] A. Rara, K. Roubik, T. Tyll, "Effects of pleural effusion drainage in the mechanically ventilated patient as monitored by electrical impedance tomography and end-expiratory lung volume: A pilot study," *J. Crit. Care*, vol. 59, pp. 76-80, 2020, doi: <https://doi.org/10.1016/j.jcrc.2020.06.001>
- [19] S. Milne, J. Huvanandana, C. Nguyen, J. M. Duncan, et al., "Time-based pulmonary features from electrical impedance tomography demonstrate ventilation heterogeneity in chronic obstructive pulmonary disease," *J. Appl. Physiol.*, vol. 127, no. 5, pp. 1441-1452, 2019, doi: <https://doi.org/10.1152/jap-physiol.00304.2019>
- [20] C. Karagiannidis, A. D. Waldmann, P. L. Róka, T. Schreiber, S. Strassmann, W. Windisch, S. H. Böhm, "Regional expiratory time constants in severe respiratory failure estimated by electrical impedance tomography: a feasibility study," *Crit. Care*, vol. 22, no. 1, art. no. 221, 2018, doi: <https://doi.org/10.1186/s13054-018-2137-3>
- [21] B. Vogt, Z. Zhao, P. Zabel, N. Weiler, I. Frerichs, "Regional lung response to bronchodilator reversibility testing determined by electrical impedance tomography in chronic obstructive pulmonary disease," *Am. J. Physiol Lung Cell Mol. Physiol.*, vol. 311, no. 1, pp. L8-L19, 2016, doi: <https://doi.org/10.1152/ajplung.00463.2015>
- [22] B. De Lema, P. Casan, P. Riu, "Electrical impedance tomography: standardizing in the procedure in pneumology," *Arch. Bronconeumol.*, vol. 42, pp. 299-301, 2006, doi: [https://doi.org/10.1016/s1579-2129\(06\)60146-8](https://doi.org/10.1016/s1579-2129(06)60146-8)
- [23] J. Fornos Herrando, "Estimació del Patró Ventilatori mitjanç, ant Tomografia d'Impedància Elèctrica," Bachelors dissertation, Universitat Politècnica de Catalunya, Catalunya, Spain, 2006.
- [24] D. B. Geselowitz, "An application of electrocardiographic lead theory to impedance plethysmography," *IEEE Trans. Biomed. Eng.*, vol. BME-18, no. 1, pp. 38-41, 1971, doi: <https://doi.org/10.1109/TBME.1971.4502787>
- [25] O. Casas, "Contribución a la obtención de imágenes paramétricas en tomografía de impedancia eléctrica para la caracterización de tejidos biológicos," Ph.D. dissertation, Universitat Politècnica de Catalunya, Catalunya, Spain, 1998.
- [26] A. Fontova, "Desenvolupament d'un mòdul de comunicacions Ethernet per a un sistema de TIE," Bachelors dissertation, Universitat Politècnica de Catalunya, Catalunya, Spain, 2004.
- [27] R. E. Serrano, B. De Lema, O. Casas, T. Feixas, et al., "Use of electrical impedance tomography (TIE) for the assessment of unilateral pulmonary function," *Physiol. Meas.*, vol. 23, art. no. 211, 2002, doi: <https://doi.org/10.1088/0967-3334/23/1/322>
- [28] O. Casas, J. Rosell, R. Bragós, A. Lozano, P. J. Riu, "A parallel broadband real-time system for electrical impedance tomography," *Physiol. Meas.*, vol. 17, art. no. A1, 1996, doi: <https://doi.org/10.1088/0967-3334/17/4A/002>
- [29] MedGraphics Products. "Technical specifications." MedGraphics Products. [http://www.sanomed.ee/Images/Med\\_Graph/CPFSDusbSpiro.pdf](http://www.sanomed.ee/Images/Med_Graph/CPFSDusbSpiro.pdf) (accessed Sept. 7, 2023).
- [30] J. Vestbo, S. S. Hurd, A. G. Agustí, P. W. Jones, et al., "Global strategy for the diagnosis, management, and prevention of chronic obstructive pulmonary disease: GOLD executive summary," *Am. J. Resp. Crit. Care*, vol. 187, no. 4, pp. 347-365, 2013, doi: <https://doi.org/10.1164/rccm.201204-0596PP>
- [31] G. Ntritsos, J. Franek, L. Belbasis, M. A. Christou, et al., "Gender-specific estimates of COPD prevalence: a systematic review and meta-analysis," *Int. J. Chronic Obstr.*, vol. 13, pp. 1507-1514, 2018, doi: <https://doi.org/10.2147%2FCOPD.S146390>
- [32] P. P. Rickham, "Human experimentation. Code of ethics of the world medical association. Declaration of Helsinki," *Brit. Med. J.*, vol. 2, no. 5402, art. no. 177, 1964, doi: <https://doi.org/10.1136/bmj.2.5402.177>
- [33] F. García-Río, M. Calle, F. Burgos, P. Casan, et al., "Espirometría," *Arch. Bronconeumol.*, vol. 49, no. 9, pp. 388-401, 2013, doi: <https://doi.org/10.1016/j.arbr.2013.07.007>
- [34] J. M. Haynes, "Basic spirometry testing and interpretation for the primary care provider," *Can. J. Respir. Ther.*, vol. 54, no. 4, pp. 92-98, 2018, doi: <https://doi.org/10.29390/cjrt-2018-017>

- [35] J. A. Neder, S. Andreoni, A. Castelo-Filho, L. E. Nery, "Reference values for lung function tests: I. Static volumes," *Braz. J. Med. Biol. Res.*, vol. 32, no. 6, pp. 703-717, 1999, doi: <https://doi.org/10.1590/S0100-879X1999000600006>
- [36] N. Macintyre, R. O. Crapo, G. Viegi, D. C. Johnson, et al., "Standardization of the single breath determination of carbon monoxide uptake in the lung," *Eur. Respir. J.*, vol. 26, pp. 720-735, 2005, doi: <https://doi.org/10.1183/09031936.05.00034905>
- [37] L. Gattinoni, A. Pesenti, M. Matthay, Understanding blood gas analysis, *Intens. Care Med.* vol. 44, no. 1, pp. 91-93, 2018, doi: <https://doi.org/10.1007/s00134-017-4824-y>
- [38] M. Balleza-Ordaz, E. Alday-Perez, M. Vargas-Luna, S. Kashina, M. R. Huerta-Franco, L. A. Torres-González, P. J. Riu-Costa, "Tidal volume monitoring by a set of tetrapolar impedance measurements selected from the 16-electrodes arrangement used in electrical impedance tomography (EIT) technique. Calibration equations in a group of healthy males," *Biomed. Signal Process. Control*, vol. 27, pp. 68-76, 2016, doi: <https://doi.org/10.1016/j.bspc.2016.02.001>
- [39] M. Balleza-Ordaz, R. Estrella-Cerón, T. Romero-Muñiz, M. Vargas-Luna, "Lung ventilation monitoring by electrical bioimpedance technique using three different 4-electrode thoracic configurations: Variability of calibration equations," *Biomed. Signal Process. Control*, vol. 47, pp. 401-412, 2019, doi: <https://doi.org/10.1016/j.bspc.2018.08.032>
- [40] J. Karsten, T. Stueber, N. Voigt, E. Teschner, H. Heinze, "Influence of different electrode belt positions on electrical impedance tomography imaging of regional ventilation: a prospective observational study," *Crit. Care*, vol. 20, art. no. 3, 2015, doi: <https://doi.org/10.1186/s13054-015-1161-9>
- [41] S. Krueger-Ziolek, B. Schullcke, J. Kretschmer, U. Müller-Lisse, K. Möller, Z. Zhao, "Positioning of electrode plane systematically influences EIT imaging," *Physiol. Meas.*, vol. 36, art. no. 1109, 2015, doi: <https://doi.org/10.1088/0967-3334/36/6/1109>
- [42] E. Szczygieł, K. Zielonka, S. Mętel, J. Golec, "Musculo-skeletal and pulmonary effects of sitting position-a systematic review," *Ann. Agric. Environ. Med.*, vol. 24, no. 1, pp. 8-12, 2017, <https://doi.org/10.5604/12321966.1227647>
- [43] S. W. Smith, *The Scientist and Engineer's Guide to Digital Signal Processing*, 2nd ed., San Diego, CA, USA: California Technical Publishing, 1999.
- [44] M. Weeks, *Digital signal processing using MATLAB and wavelets*, 1st ed., Hingham, MA, USA: Infinity Science Press LLC, 2007.
- [45] M. Ghita, D. Copot, M. Ghita, E. Derom, C. Ionescu, "Low Frequency Forced Oscillation Lung Function Test Can Distinguish Dynamic Tissue Non-linearity in COPD Patients," *Front. Physiol.*, vol. 10, art. no.1390, 2019, doi: <https://doi.org/10.3389/fphys.2019.01390>